

Supporting Information

Exploring the Slow Magnetic Relaxation of a Family of Photoluminescent 3D Lanthanide-Organic Frameworks Based on Dicarboxylate Ligands

Itziar Oyarzabal, Sara Rojas, Ana D. Parejo, Alfonso Salinas-Castillo, José Ángel García, José M. Seco, Javier Cepeda and Antonio Rodríguez-Diéguez

Index:

1. Powder X-ray Diffraction
2. Additional structural data
3. Interpretation of void content from SQUEEZE analysis
4. Continuous Shape Measures Calculations
5. Magnetic Properties
6. Luminescence Properties

S1. Powder X-ray Diffraction

Table S1. Data of pattern-matching refinement of compound **2**.

Space group	<i>P-1</i>
<i>a</i> (Å)	10.87(2)
<i>b</i> (Å)	11.11(2)
<i>c</i> (Å)	13.26(3)
α (°)	105.28(2)
β (°)	94.22(3)
γ (°)	93.65(2)
<i>V</i> / Å ³	1534(3)

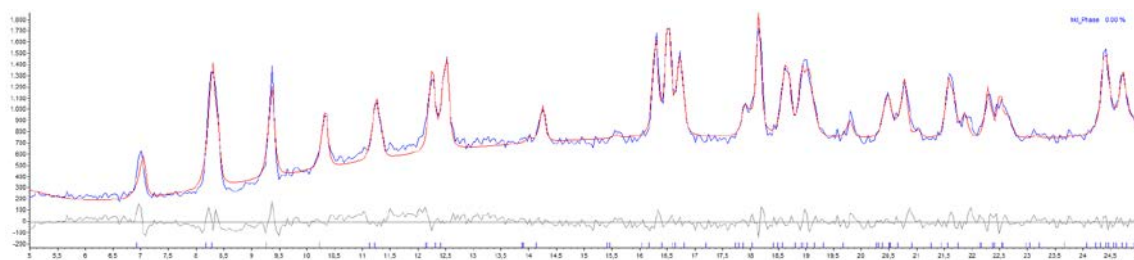


Figure S1. Pattern-matching analysis and crystalline parameters of the polycrystalline sample of compound **2**.

Table S2. Data of pattern-matching refinement of compound **3**.

Space group	<i>P-1</i>
<i>a</i> (Å)	10.85(2)
<i>b</i> (Å)	11.04(4)
<i>c</i> (Å)	13.21(2)
α (°)	105.01(2)
β (°)	94.90(4)
γ (°)	93.90(4)
<i>V</i> / Å ³	1516(5)

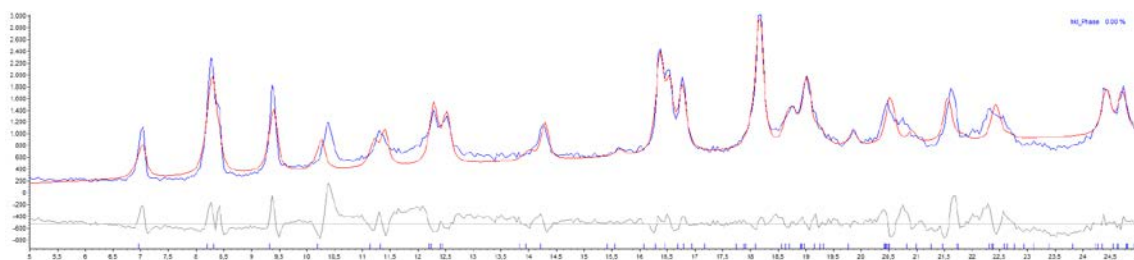


Figure S2. Pattern-matching analysis and crystalline parameters of the polycrystalline sample of compound **3**.

Table S3. Data of pattern-matching refinement of compound **4**.

Space group	<i>P</i> -1
<i>a</i> (Å)	10.86(2)
<i>b</i> (Å)	11.03(4)
<i>c</i> (Å)	13.20(2)
α (°)	105.20(2)
β (°)	94.38(4)
γ (°)	93.75(4)
<i>V</i> /Å ³	1515(5)

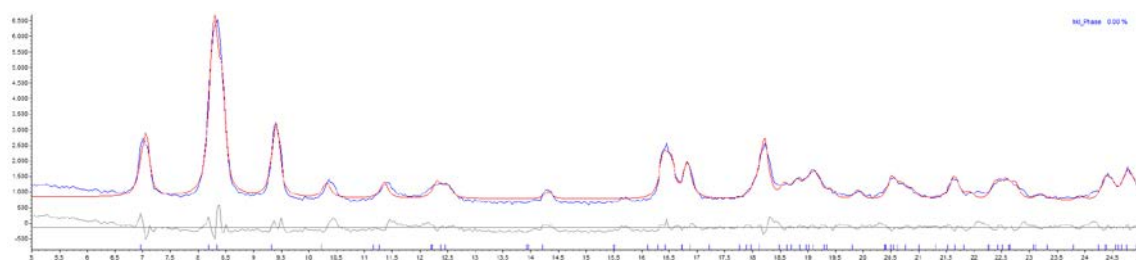


Figure S3. Pattern-matching analysis and crystalline parameters of the polycrystalline sample of compound **4**.

S2. Additional structural data

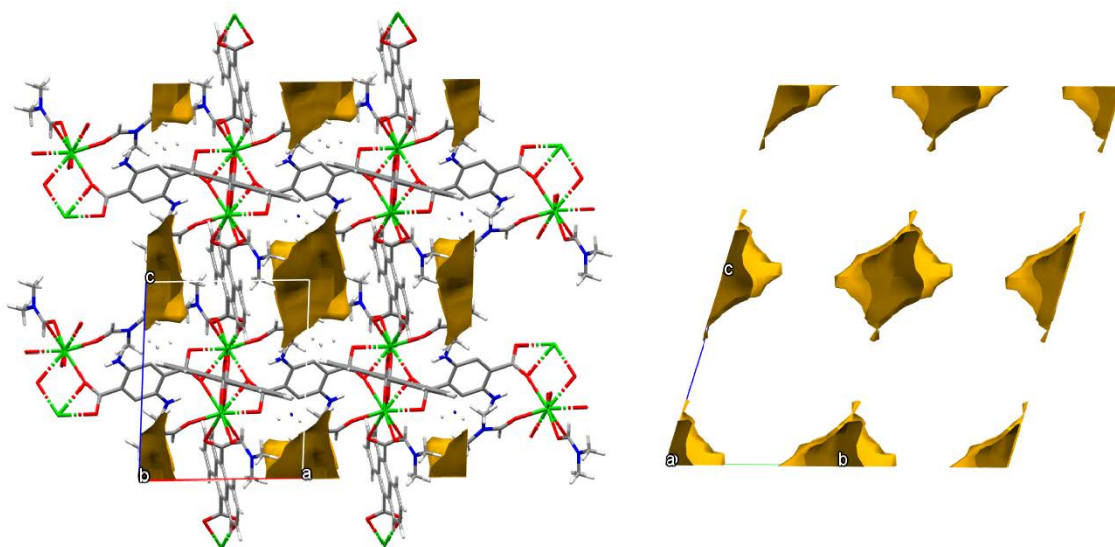


Figure S4. Captures of the 3D framework of compound **1** showing the voids present that are occupied by lattice DMF molecules. Two different views are shown: along *b* axis (left) and along *a* axis (right).

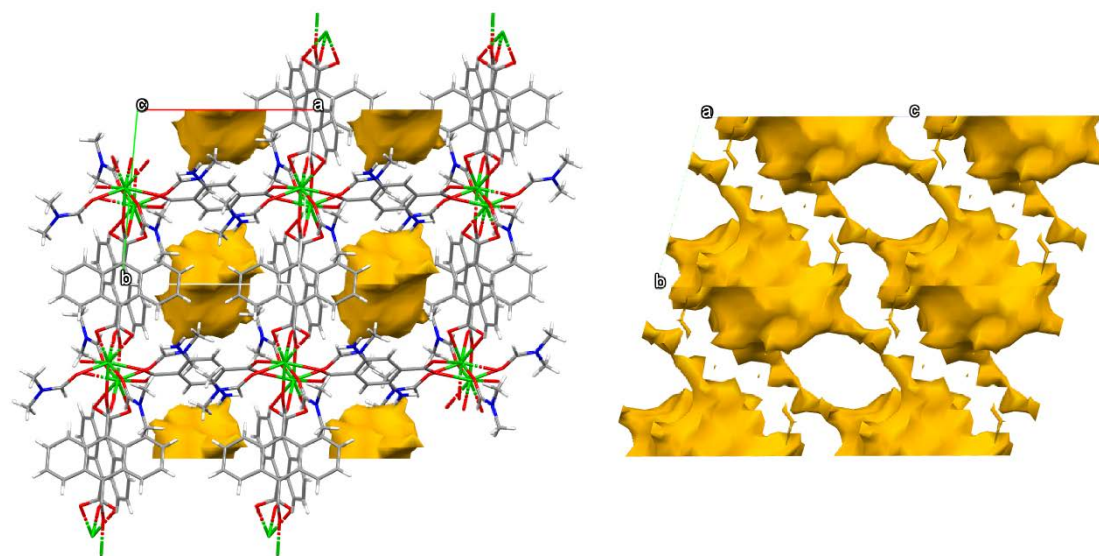


Figure S5. Captures of the 3D framework of compounds **2-4** showing the connected voids present. Two different views are shown: along *c* axis (left) and along *a* axis (right).

S3. Interpretation of void content from SQUEEZE analysis.

Compound **1** consists of a MOF structure that contains lattice solvent molecules that crystallize in a highly disordered arrangement so as to be correctly solved. Therefore, the final refinement was performed with SQUEEZE routine and used to calculate the void space and the electron count. The report shows that the void content is of 296 Å³ and 85 electrons, so taking into account that $Z = 2$ in this crystal structure, and that DMF was used as solvent, it may be assumed that the voids contain 1 DMF molecule per formula unit.

S4. Continuous Shape Measures Calculations

Table S4. Continuous Shape Measures Calculations for herein described compound **1**, and previously reported $\{[\text{Nd}(\text{ant})_{1.5}(\text{DMF})_2] \cdot (\text{DMF})\}_n$, $\{[\text{Dy}(\text{ant})_{1.5}(\text{DMF})_2] \cdot (\text{DMF})\}_n$ and $\{[\text{Dy}_2(\text{ant})_2((\text{NH}_2)_2\text{-bdc})(\text{DMF})_4] \cdot 2\text{DMF} \cdot 2\text{H}_2\text{O}\}_n$ [1].

EP-9	1 D9h	Enneagon
OPY-9	2 C8v	Octagonal pyramid
HBPY-9	3 D7h	Heptagonal bipyramid
JTC-9	4 C3v	Johnson triangular cupola J3
JCCU-9	5 C4v	Capped cube J8
CCU-9	6 C4v	Spherical-relaxed capped cube
JCSAPR-9	7 C4v	Capped square antiprism J10
CSAPR-9	8 C4v	Spherical capped square antiprism
JTCTPR-9	9 D3h	Tricapped trigonal prism J51
TCTPR-9	10 D3h	Spherical tricapped trigonal prism
JTDIC-9	11 C3v	Tridiminished icosahedron J63
HH-9	12 C2v	Hula-hoop
MFF-9	13 Cs	Muffin

	EP-9	OPY-9	HBPY-9	JTC-9	JCCU-9	CCU-9	JCSAPR-9
Compound 1	33.434	23.029	14.845	15.317	10.405	8.982	3.912
$\{[\text{Nd}(\text{ant})_{1.5}(\text{DMF})_2] \cdot (\text{DMF})\}_n$	34.783	21.924	15.736	15.076	10.725	9.232	2.904
$\{[\text{Dy}(\text{ant})_{1.5}(\text{DMF})_2] \cdot (\text{DMF})\}_n$	34.945	21.692	16.081	15.053	10.692	9.178	2.629

	CSAPR-9	JTCTPR-9	TCTPR-9	JTDIC-9	HH-9	MFF-9
Compound 1	2.658	4.719	3.195	12.344	8.281	2.251
$\{[\text{Nd}(\text{ant})_{1.5}(\text{DMF})_2] \cdot (\text{DMF})\}_n$	2.052	4.937	2.449	12.596	8.906	1.835
$\{[\text{Dy}(\text{ant})_{1.5}(\text{DMF})_2] \cdot (\text{DMF})\}_n$	1.858	4.628	2.338	12.484	8.935	1.675

Table S5. Continuous Shape Measures Calculations for the isostructural Dy-based analogue [1] of compounds **2–4** due to the lack of single crystals of these specimens. The Tb (**2**), Ho (**3**) and Er (**4**) compounds are expected to have similar coordination environments to that of Dy in both materials.

OP-8	1 D8h	Octagon
HPY-8	2 C7v	Heptagonal pyramid
HBPY-8	3 D6h	Hexagonal bipyramid
CU-8	4 Oh	Cube
SAPR-8	5 D4d	Square antiprism
TDD-8	6 D2d	Triangular dodecahedron
JGBF-8	7 D2d	Johnson gyrobifastigium J26
JETBPY-8	8 D3h	Johnson elongated triangular bipyramid J14
JBTPR-8	9 C2v	Biaugmented trigonal prism J50
BTPR-8	10 C2v	Biaugmented trigonal prism
JSD-8	11 D2d	Snub diphenooid J84
TT-8	12 Td	Triakis tetrahedron
ETBPY-8	13 D3h	Elongated trigonal bipyramid

	OP-8	HPY-8	HBPY-8	CU-8	SAPR-8	TDD-8	JGBF-8
$\{[\text{Dy}_2(\text{ant})_2((\text{NH}_2)_2\text{-bdc})(\text{DMF})_4] \cdot 2\text{DMF} \cdot 2\text{H}_2\text{O}\}_n$	31.338	23.048	14.547	9.578	1.869	1.901	13.598

	JETBPY-8	JBTPR-8	BTPR-8	JSD-8	TT-8	ETBPY-8
$\{[\text{Dy}_2(\text{ant})_2((\text{NH}_2)_2\text{-bdc})(\text{DMF})_4] \cdot 2\text{DMF} \cdot 2\text{H}_2\text{O}\}_n$	26.173	2.006	1.418	4.198	10.246	21.957

S5. Magnetic Properties

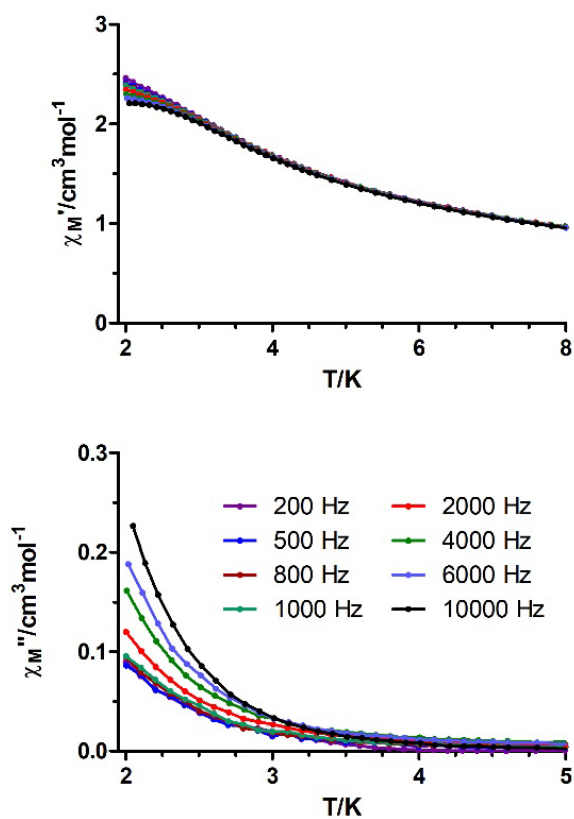


Figure S6. Temperature dependence of the in-phase (top) and out-of-phase (bottom) components of the *ac* susceptibility for **4** under an external field of 1000 Oe (the susceptibility values are given per Er(III) ion).

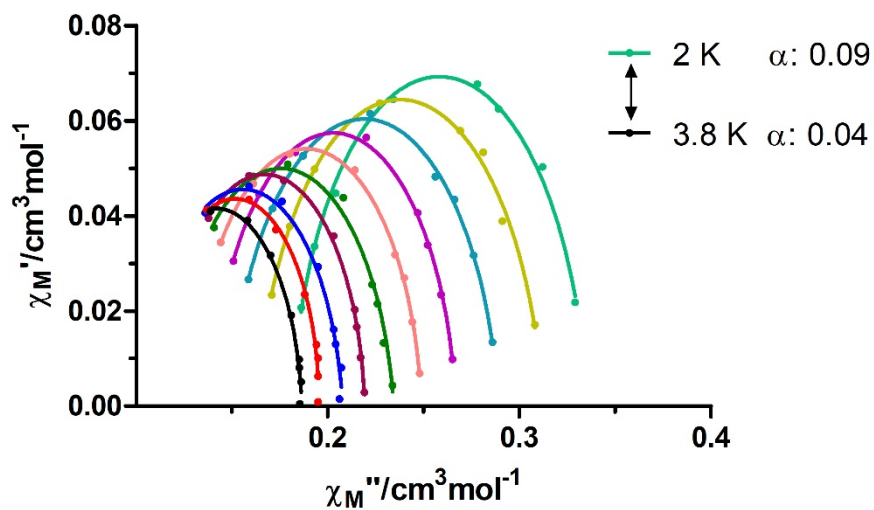


Figure S7. Cole-Cole plots under 1000 Oe external field for **1**. Solid lines represent the best fits to the generalized Debye model.

S5. Luminescence Measurements

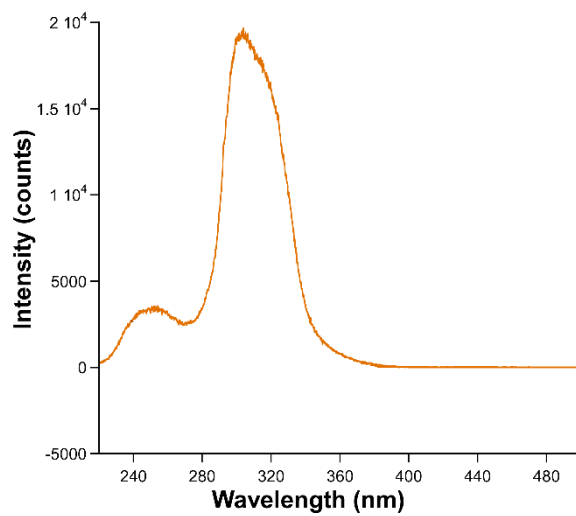


Figure S8. Excitation spectrum of compound **2** measured at room temperature at $\lambda_{em} = 548$ nm.

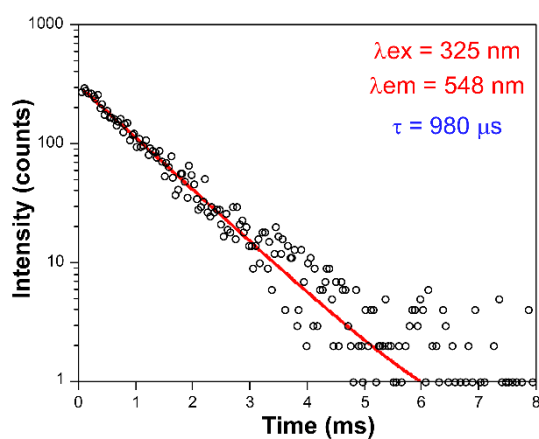


Figure S9. Excitation spectrum of compound **2** measured at room temperature at $\lambda_{em} = 548$ nm.

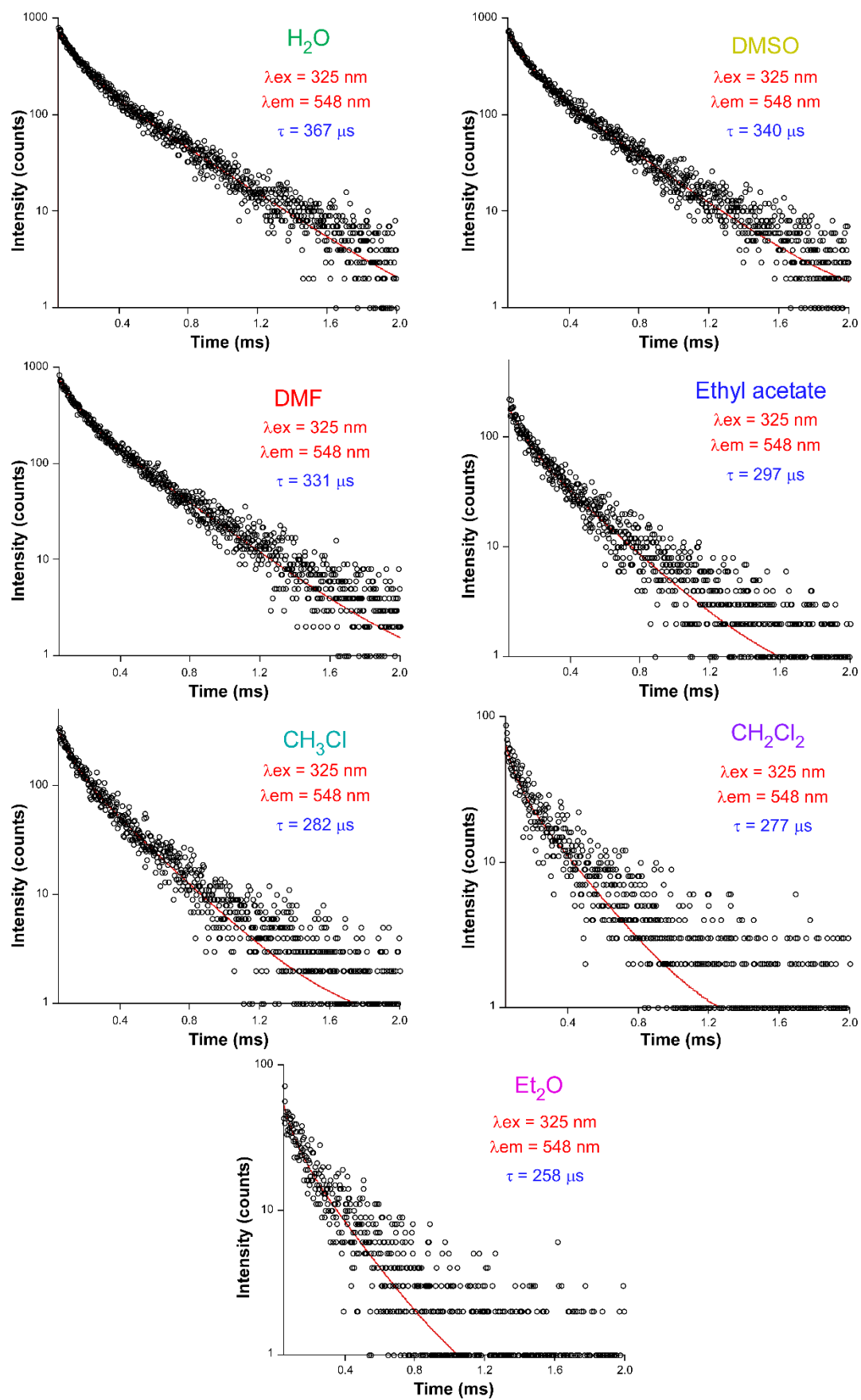


Figure S10. Decay curves of compound 2 acquired on dispersions of different solvents (see specified conditions).

1. Oyarzabal, I.; Fernández, B.; Cepeda, J.; Gómez-Ruiz, S.; Calahorra, A.J.; Seco, J.M.; Rodríguez-Diéguez, A. Slow relaxation of magnetization in 3D-MOFs based on dysprosium dinuclear entities bridged by dicarboxylic linkers. *CrystEngComm* **2016**, *18*.